

Hongxin Su · Jan C. Axmacher · Bo Yang  
Weiguo Sang

## Differential radial growth response of three coexisting dominant tree species to local and large-scale climate variability in a subtropical evergreen broad-leaved forest of China

Received: 15 August 2014 / Accepted: 30 April 2015 / Published online: 16 May 2015  
© The Ecological Society of Japan 2015

**Abstract** Subtropical evergreen broad-leaved forests (EBF) face great pressure from global climate change. However, little consensus exists related to how coexisting trees in these forests will respond to climatic change. We used tree rings to establish climate-growth relationships of three coexisting dominant canopy tree species in an EBF located in the Gutianshan National Nature Reserve, Zhejiang Province, in eastern China. Our results emphasize highly species-specific radial growth responses to both local and large-scale climate variability. The radial growth of *Pinus massoniana* was enhanced by high minimum autumn and low winter temperatures as well as La Niña events. Positive growth responses in *Castanopsis eyrei* were linked to high minimum summer and spring temperatures. Low winter temperatures and summer sunshine also increased the growth of *Schima superba*. We modeled future tree-ring growth using two climate change scenarios. Under both an intermediate (Representative Concentration Pathway, RCP 4.5) and a high emission climate change scenario (RCP 8.5), we projected further growth acceleration in *C. eyrei*, but a reduced growth rate in *S. superba*. Growth of *P. massoniana* was not predicted to change under the RCP 4.5 scenario, but was predicted to

increase significantly under the RCP 8.5 scenario. These results suggest that climate change will have repercussions for the competitive balance among these tree species in subtropical forests, and the diverging responses of individual tree species need to be fully considered in any models of the effects of climate change on the EBF and in future management plans.

**Keywords** Asian monsoon · Dendrochronology · El Niño-Southern Oscillation · Evergreen broadleaved forest · Representative concentration pathways

### Introduction

Forest ecosystems play a major role in the terrestrial carbon cycle, with an increasing biomass of trees acting as an important potential carbon sink (Pan et al. 2011). Actual tree growth rates are constrained by environmental stressors that also limit the overall capacity of forests to store carbon (Ashton et al. 2012). Models simulating forest growth responses to climate change therefore require an in-depth understanding of the effect of climatic stressors particularly on dominant tree species (He et al. 2005; Way and Oren 2010; Galvan et al. 2014). Tree species that dominate during different successional stages, precipitation regimes or ranges of elevation can be expected to differ in their responses to variations in climate (Miyamoto et al. 2010; Babst et al. 2013; Huang et al. 2013; Subedi and Sharma 2013) based on their specific resource and habitat requirements (May 1974). This adds substantial complexity to the modeling of forest dynamics especially in species-rich forest ecosystems (Anderson-Teixeira et al. 2013).

Evergreen broad-leaved forests (EBF) form an important regional vegetation type in subtropical eastern Asia (Kira 1991). These forests are particularly widespread in the subtropics of China because of the combined climatic influence of the Tibet Plateau and the

**Electronic supplementary material** The online version of this article (doi:10.1007/s11284-015-1276-0) contains supplementary material, which is available to authorized users.

H. Su · B. Yang · W. Sang (✉)  
State Key Laboratory of Vegetation and Environmental Change,  
Institute of Botany, Chinese Academy of Sciences, Beijing 100093,  
China  
E-mail: swg@ibcas.ac.cn  
Tel.: +86-10-82599519

J. C. Axmacher  
UCL Department of Geography, University College London,  
Pearson Building, Gower Street, London WC1E 6BT, UK

B. Yang  
Key Laboratory of Specialty Plant Resources of Jiangxi Province,  
Jingdezhen University, Jingdezhen 333000, China

Asian monsoon (Wu 1980). These EBF are of great interest as they relate to the conservation of biodiversity because they harbor a rich diversity of woody species similar to that of many tropical forests (Wills et al. 2006; Legendre et al. 2009). In addition, they form a significant global carbon sink (Tan et al. 2011; Li et al. 2012; Yu et al. 2014). However, EBFs face great pressures from both human disturbance and climate change (Wang et al. 2007). Within China, where forest protection has greatly improved during recent decades, climate change now serves as the main driver of EBF ecosystem dynamics (Zhou et al. 2013). Recent progress has been made in assessing the effects of climate change on functional groups, tree growth and the resulting carbon budget of EBFs at community and ecosystem scales (Tan et al. 2012; Yan et al. 2013; Zhou et al. 2013). However, little consensus exists as it relates to the response of coexisting trees in an ESF to the changing environment, which is a critical component for the prediction of future community composition and consequent ecosystem functioning; this also has broad implications related to the management of EBF ecosystems.

Tree ring analysis provides a very effective tool that can be used to determine the variability in annual tree growth, allowing an assessment of climate-change related growth responses at the individual and population levels (Williams et al. 2010; Liu et al. 2013; Takahashi and Okuhara 2013; Girard et al. 2014). Dendrochronological studies in subtropical regions have shown that radial tree growth is sensitive to changes in precipitation rates (Morales et al. 2004) and air temperature (Duan et al. 2012; Zheng et al. 2012), as well as generally climatic variability at regional and large-scales (Barichivich et al. 2009; Chen et al. 2012; Guan et al. 2012). However, to our knowledge no study has assessed the differential response of coexisting dominant tree species to climate change in an EBF and quantified the respective relative importance of local and large-scale climatic variability on each species' growth. As a consequence, uncertainties in the responses of patterns of tree growth will continue to challenge long-term forest simulations until the effects of the different climatic drivers are fully understood.

In this study, we measured tree ring data from three coexisting, dominant canopy tree species with differing shade tolerance in an old-growth EBF located in eastern China. Our primary objective was to investigate how these coexisting trees differ in their response in radial growth to local and large-scale climatic variability over the last five decades. In our analysis, we explicitly include relationships between large-scale climatic drivers and local climate variability to unravel the direct and indirect effects of large-scale climatic forces on tree growth. A second objective of this study was to develop statistical models that can be used for predicting tree-ring widths of the three tree species analyzed here, and to investigate the potential effects of climate change on the growth of these species in the future.

## Materials and methods

### Study site and sampling

The study was conducted in the Gutianshan National Nature Reserve in the west of Kaihua County, Zhejiang Province, East China ( $29^{\circ}10'19.4''$ – $29^{\circ}17'41.4''$ N,  $118^{\circ}03'49.7''$ – $118^{\circ}11'12.2''$ E). This reserve was designated for the preservation of typical old-growth EBF in China's mid-subtropical region and is characterized by steep granite mountains. The dominant soil is Ultisol, a subtropical red soil, according to the US soil taxonomy. Nearby the Kaihua weather station ( $29^{\circ}08'04''$ N,  $118^{\circ}24'07.5''$ E, 143 m a.s.l.) has recorded a mean annual temperature of  $16.4 \pm 0.5$  °C (monthly means of  $4.7 \pm 1.4$  °C in January and  $27.6 \pm 0.9$  °C in July) and a mean annual precipitation of  $1793.1 \pm 359.3$  mm (Fig. 1). The area experiences wet summer and dry winter conditions, leading to the production of distinct annual tree rings in many tree species.

The three ring-producing tree species (Song et al. 2011; Xing et al. 2012) selected for our investigation are all widespread in subtropical eastern China and vary in their successional status and respective shade tolerance. *Pinus massoniana* is a fast-growing, evergreen, sun-loving pioneer conifer species, while *Castanopsis eyrei* is an evergreen broad-leaved tree of intermediate shade-tolerance and *Schima superba* is a late successional, shade-tolerant evergreen broadleaved species found primarily in mature forests. According to data from a 24-ha forest dynamics plot in the vicinity of our study area, the three selected species account for a combined 64.1 % of the total stem area (measured at breast height, 33.9 % for *C. eyrei*, 18.9 % for *S. superba* and 11.5 % for *P. masso-*

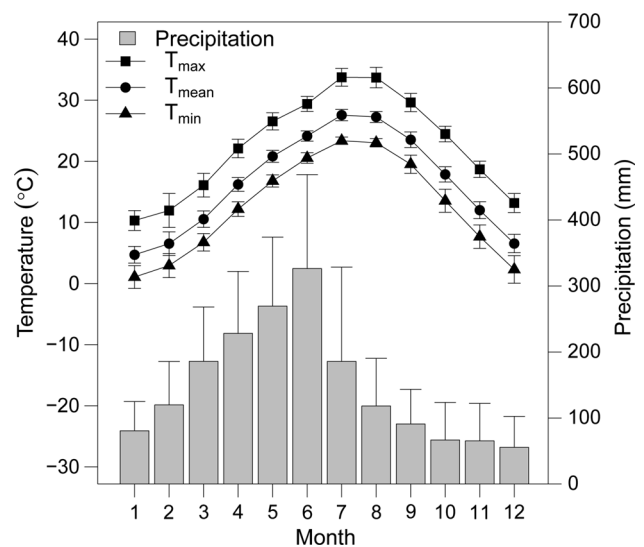


**Fig. 1** Climate of the research area (data from the Kaihua weather station covering the period between 1958 and 2010).  $T_{\min}$ ,  $T_{\text{mean}}$ , and  $T_{\text{max}}$  represent the average monthly minimum, mean, and maximum temperatures, respectively. Error bars indicate standard deviation

*niana*, respectively) in the community (Zhu et al. 2008), reflecting their dominance in the EBF canopy. The individual trees selected for sampling grew in close vicinity to a 24-ha permanent forest plot. Increment core samples were collected at breast height in the perpendicular direction of the slope from individual trees showing no sign of obvious rot or damage to the stem. For our study, we cored a total of 137 trees from the three target tree species in November 2008 under a permit from the Gutianshan National Nature Reserve Management Bureau.

### Sample measurements and data treatment

In the laboratory, the increment core samples were mounted, air dried and sanded with up to 600 grit sandpaper. Ring widths of the samples were measured with WinDendro WinDENDROTM 2001b apparatus (Université Du Québec À Chicoutimi, Canada) to a precision of 0.01 mm. The ring width series were cross-dated and quality checked using the COFECHA program (Holmes 1983), insuring that each ring was assigned to the correct calendar year of its formation. These series were subsequently standardized to remove age-related growth trends using the ARSTAN program (Cook 1985), in which the detrending curve selected was a negative exponential curve, a horizontal line, or a straight line with negative slope. A standard tree-ring chronology for each species was developed by averaging the standardized tree-ring series among the individuals (Fritts 1976).

### Climatic data

The El Niño-Southern Oscillation (ENSO) provides one of the main sources of variability in global climatic conditions, and has a very strong effect on the Asian monsoon and the associated local climate patterns in subtropical China. ENSO events are described by the Multivariate ENSO Index (MEI; Wolter and Timlin 2011). A positive MEI value represents an El Niño event, while a negative value corresponds to a La Niña episode. Bimonthly values of the MEI for the period of 1958–2008 were obtained from the NOAA Earth System Research Laboratory (<http://www.esrl.noaa.gov/psd/enso/mei/>). In our investigations, we used the average value of the MEI from the previous December to the current November period as the respective annual value for the current year.

The Asian monsoon represents the most important regional driving factor affecting the climatic dynamics in subtropical China. Two distinct sub-systems make up this monsoon, the East Asian (EAM) and the South Asian summer (SASM) monsoons. The East Asian winter monsoon (EAWM) results in strong northerly winds in winter and the East Asian summer monsoon (EASM) results in strong southerly winds in summer. The EAWM index represents the intensity of the winter monsoon (Guo 1994), and data for this index covering

the period from 1958 to 2008 was provided by the National Climate Center of the China Meteorological Administration. For the same period, we also downloaded the EASM and SASM indices (Li and Zeng 2002, 2003) from <http://ljp.gcess.cn/dct/page/1>.

For local historical climate data, monthly data including precipitation (mm), temperature (°C), relative humidity (%) and percentage sunshine (%) were obtained from the Kaihua weather station for the period of 1958–2008. Monthly data were used to calculate mean seasonal values as follows: winter (December–February), spring (March–May), summer (June–August), and autumn (September–November). Annual mean values were then calculated as averages for the period from December of the last year to November of the current year, because delineation based on the four seasons appeared to be most appropriate.

For the projected monthly local climatic data from 2009 to 2099, including the average daily temperature, daily maximum and minimum temperatures, total precipitation and percentage of sunshine, we used simulations from nine Global Climate Models (GCM) selected from the Coupled Model Intercomparison Project Phase 5 (CMIP5) under a high emission scenario (Representative Concentration Pathways 8.5, RCP8.5) and an intermediate emission scenario (RCP4.5; Fig. 2, Moss et al. 2010; Taylor et al. 2012; for details see Supplemental Information).

In addition, results from the CMIP5 showed that the change in ENSO amplitude from the 20th century value is statistically insignificant between most RCP ensembles for the 21st century (Stevenson et al. 2012, 2013). The effects of climate change on future ENSO variability remains largely unknown and unforced ENSO modulations are substantial. This makes it extremely difficult to simulate future ENSO teleconnections in the GCM (Weare 2013; Bellenger et al. 2014). Hence, the MEI for the future (2009–2099) was assumed to be the same as recorded in the historical observations for the corresponding 20th century period (1909–1999) (<http://www.esrl.noaa.gov/psd/enso/mei/>).

### Climate-growth analyses

The influence of the precipitation, temperature, relative humidity and percentage of sunshine on radial growth was established at monthly, seasonal and annual time-scales to identify the most suitable explanatory variables for the local climate. The response function and Pearson correlation analysis of monthly data potentially best represents responses of the three tree species to climatic variables. However, the analysis of monthly data leads to a wealth of climatic parameters, which can increase noise in the predictors and add uncertainty in the final model; in contrast, correlation analysis of annual mean parameters allows a very coarse analysis widely neglecting interannual variations (please see the Supplemental Information for details). An analysis of growth

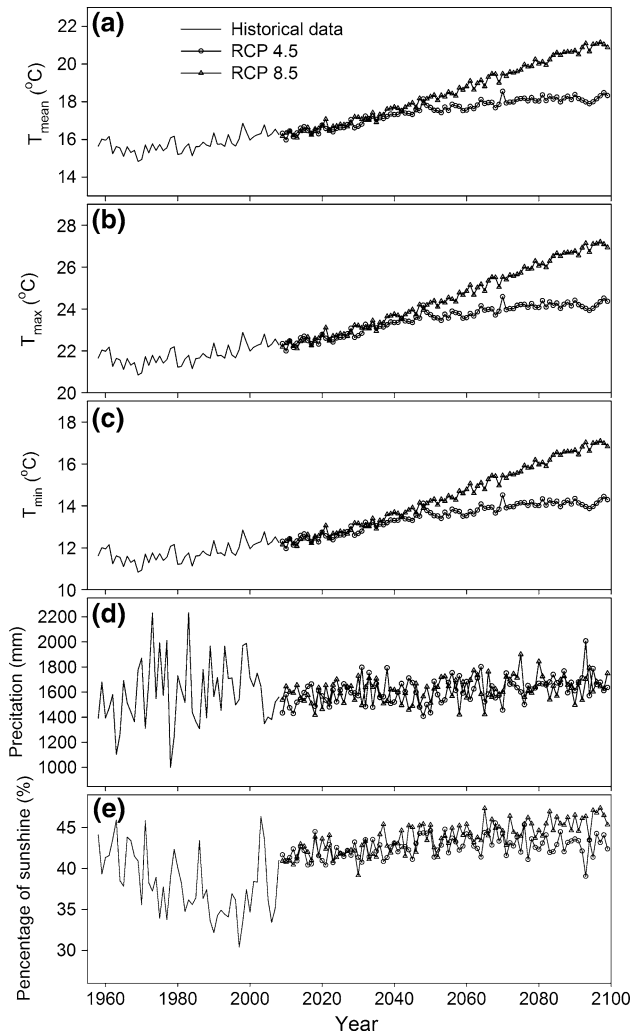


**Fig. 2** Time series of annual mean temperature ( $T_{\text{mean}}$ ), maximum temperature ( $T_{\text{max}}$ ), minimum temperature ( $T_{\text{min}}$ ), precipitation and percentage of sunshine for the Gutianshan National Nature Reserve from 1958 to 2099 as basis for the multi-model ensemble. *RCP4.5* Representative Concentration Pathway 4.5, *RCP8.5* Representative Concentration Pathway 8.5

responses to seasonal climatic variations in this regard provides a strong compromise. The Akaike Information Criterion (AIC) was used to obtain the best set of predictors for the forward regression models used to describe tree ring growth of the three target tree species.

Based on this model selection, a path analysis was used to establish the influence of both, large-scale climatic drivers (ENSO and Asian monsoon) and local climatic variations on tree growth (Brienen et al. 2010). All possible paths from large-scale climatic drivers to the selected local climate factors, from large scale climatic drivers to tree growth, and from the selected local climate factors to tree growth were established, including non-significant links to illustrate all underlying relationships. This approach can potentially reduce the statistical reliability of the model, because the number of paths is relatively large compared to the sample size, but

results did not change when we reduced the number of relations by removing all non-significant paths (Kline 2010). In this analysis, direct effects ( $r_{\text{direct}}$ ) consisted of direct relationships between a large-scale climate index and tree growth. Indirect effects ( $r_{\text{indirect}}$ ) were interpreted to occur when a climate index could only be correlated with tree growth through its correlation with a local climate effect. The magnitude of indirect effects was then compared to direct effects by calculating standardized coefficients for each path. Total effects ( $r_{\text{total}}$ ) were calculated as the sum of the direct and indirect effects.

### Growth projections for 2009–2099

In this study, we predict future tree-ring growth using a climatic change scenario and the present growth-climate relationships of the three target tree species (Takahashi and Okuhara 2013). Based on the path analyses, a multiple regression model was developed based on past large-scale climatic drivers, selected local climatic factors and the tree-ring width indices of each tree species. These models were statistically verified following the methods of Takahashi and Okuhara (2013; see Supplemental Information for details). This study assumes that growth-climate relationships did not change with time (or climatic changes) and analyzed the radial growth forecast by substituting future climatic change scenarios into the growth response models. All statistical analyses were performed using R (R Development Core Team 2011).

## Results

### Tree ring chronologies and growth patterns

The length of the chronologies varied from 80 to 110 years, with the longest chronology dating back to 1899 for *P. massoniana* (Table 1). During the common reliable period of each chronology, the subsample signal strength (SSS) exceeded 0.85 and the expressed population signal (EPS) was particularly high, which shows that our samples captured 86–96 % of the inter-annual growth variation in the population. The first principal component explained 30.1–41.2 % of the total variance in the three chronologies. Temporal growth variation was similar between *P. massoniana* and *C. eyrei* ( $r = 0.41$ ,  $P = 0.003$ ) and between *P. massoniana* and *S. superba* ( $r = 0.35$ ,  $P = 0.014$ ), but differed more strongly between *C. eyrei* and *S. superba* ( $r = 0.08$ ,  $P = 0.56$ ; Fig. 3).

### Local climate and radial growth

Correlation analyses showed that the growth of *P. massoniana* was strongly enhanced by warm autumn



**Table 1** Statistical characteristics of the chronologies of three tree species analyzed here

	<i>Pinus massoniana</i>	<i>Castanopsis eyrei</i>	<i>Schima superba</i>
Total number of series	82	28	37
Full chronology interval	1899–2008	1929–2008	1922–2008
Chronology interval (SSS > 0.85)	1940–2008 (48)	1947–2008 (21)	1946–2008 (26)
Mean sensitivity	0.1905	0.1495	0.1648
Standard deviation	0.3322	0.2495	0.2961
Mean correlations among all radii	0.316	0.244	0.292
First order autocorrelation	0.7851	0.6841	0.7686
Signal-to-noise ratio	22.074	14.101	17.824
Express population signal	0.957	0.864	0.917
Variance in first eigenvector (%)	41.22	30.07	35.79

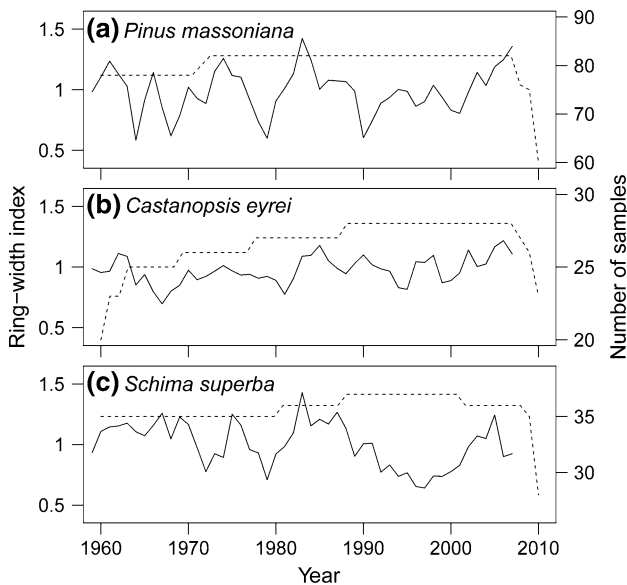


**Fig. 3** Tree ring-width chronologies (1958–2008) and number of cores sampled for *Pinus massoniana*, *Schima superba* and *Castanopsis eyrei*. Black solid lines represent the chronology, and the dashed line represents the number of cores used as the basis for the chronology

temperatures and strongly negatively affected by warm winter temperatures ( $T_{win}$ ; Table 2). Growth of *C. eyrei* was reduced when cold spells occurred in spring or summer. In contrast, *S. superba* showed a strong adverse growth reaction towards warm winter temperatures and to a lesser degree also to warm spring temperatures. In addition, warm summer temperatures and especially a large number of sunshine hours in summer ( $Sun_{sum}$ ) had a strong positive effect on growth of *S. superba*. In contrast, precipitation in the summer months triggered a significant negative growth response in this species. Stepwise forward linear regression models (Table 3), confirmed that *S. superba* growth was mainly affected by  $T_{win}$  and  $Sun_{sum}$ , while *C. eyrei* growth was limited by cold summer and spring temperatures, and *P. massoniana* growth profited chiefly from warm autumn and cold winter temperatures.

### Large-scale climate drivers and radial tree growth

The correlation analysis between growth and large-scale climatic drivers again reflected significant differences between the three species. Growth of *P. massoniana* increased significantly in La Niña years and decreased in El Niño years, while both *P. massoniana* and *S. superba* showed increased growth in strong EAWM years with their associated cold winter temperatures (Table 4). The integration of both the ENSO and the Asian monsoon with local climatic conditions is therefore seen as critical in a comprehensive analysis that can be used to predict tree growth responses under future climate change scenarios.

### Path analysis

The path diagram confirms that both large-scale climatic drivers and selected local climate factors effect tree growth, with the magnitude of direct and indirect relationships varying between species (Fig. 4). *P. massoniana* growth was directly affected by MEI ( $r_{direct} = -0.44$ ),  $T_{win}$  ( $r_{direct} = -0.37$ ) and  $T_{min(aut)}$  ( $r_{direct} = 0.43$ ), where  $T_{win}$ ,  $r_{direct}$  and  $T_{min(aut)}$  are defined as mean temperatures of winter, and mean minimum temperature of autumn. EAWM had a negative direct effect on growth, but this was partially cancelled by a stronger positive indirect effect on growth through  $T_{win}$  and  $T_{min(aut)}$ , resulting in a positive total effect ( $r_{direct} = -0.20$ ,  $r_{indirect} = 0.36$ ,  $r_{total} = 0.12$ ).

*C. eyrei* growth was directly affected by  $T_{min(spr)}$  ( $r_{direct} = 0.30$ ), and  $T_{min(sum)}$  ( $r_{direct} = 0.43$ ), where  $T_{min(spr)}$  and  $T_{min(sum)}$  are the mean minimum temperatures of spring and summer, respectively. The negative direct effect of MEI was offset by a stronger indirect positive effect ( $r_{direct} = -0.22$ ,  $r_{indirect} = 0.23$ ,  $r_{total} = 0.01$ ). SASM directly negatively affected *C. eyrei* growth, but this was again partially concealed by the positive indirect effect, and the total resulting effect was positive ( $r_{direct} = -0.18$ ,  $r_{indirect} = 0.32$ ,  $r_{total} = 0.14$ ).

*S. superba* growth was directly affected by  $T_{win}$  ( $r_{direct} = -0.39$ ), and  $Sun_{sum}$  ( $r_{direct} = 0.36$ ), where

**Table 2** Correlation between radial growth and seasonal climatic variations of the three species analyzed here

Species	Temperature			Maximum temperature			Minimum temperature			Precipitation			Sunshine percentage							
	Winter	Spring	Summer	Winter	Spring	Summer	Winter	Spring	Summer	Winter	Spring	Summer	Winter	Spring	Summer					
<i>Pinus massoniana</i>	-0.32*	0.10	0.19	0.28*	-0.21	0.20	0.17	0.01	-0.26	0.05	0.28	0.39**	-0.07	-0.14	-0.11	0.09	0.16	0.04	0.03	-0.26
<i>Castanopsis eyrie</i>	0.16	0.35*	0.20	0.10	0.11	0.28	0.06	-0.01	0.17	0.36*	0.41**	0.17	0.04	-0.19	-0.13	0.05	0.04	0.01	-0.1	-0.11
<i>Schima superba</i>	-0.56**	-0.32*	0.14	-0.10	-0.32*	-0.17	0.36*	0.02	-0.55**	-0.35*	-0.2	-0.13	-0.26	-0.02	-0.37**	0.01	0.26	0.04	0.41**	0.02

Winter, December<sub>previous year</sub>-February; Spring, March-May; Summer, June-August; Autumn, September-November  
 \*  $P < 0.05$  (2-tailed), \*\*  $P < 0.01$  (2-tailed)

**Table 3** Forward linear regression models predicting radial growth of the three tree species based on seasonal climatic variations

	$\beta$	$t$ value	$P$
<i>Pinus massoniana</i> (adjusted $R^2 = 0.22$ )			
$T_{\min(\text{atu})}$	0.425	3.347	0.002
$T_{\text{win}}$	-0.283	-2.228	0.030
$T_{\max(\text{sum})}$	0.201	1.552	0.130
<i>Castanopsis eyrei</i> (adjusted $R^2 = 0.21$ )			
$T_{\min(\text{sum})}$	0.379	2.911	0.006
$T_{\min(\text{spr})}$	0.340	2.550	0.010
$Sun_{\text{win}}$	0.228	1.712	0.090
<i>Schima superba</i> (adjusted $R^2 = 0.39$ )			
$T_{\text{win}}$	-0.473	-4.129	< 0.001
$Sun_{\text{sum}}$	0.299	2.650	0.010
$T_{\text{spr}}$	-0.166	-1.454	0.150

$T_{\min(\text{atu})}$  mean minimum temperature of autumn,  $T_{\text{win}}$  mean temperatures of winter,  $T_{\max(\text{sum})}$  mean maximum temperature of summer,  $T_{\min(\text{sum})}$  mean minimum temperature of summer,  $T_{\min(\text{spr})}$  mean minimum temperature of spring,  $T_{\text{spr}}$  mean temperatures of spring,  $Sun_{\text{win}}$  sunshine hours of winter,  $Sun_{\text{sum}}$  sunshine hours of summer

$T_{\text{win}}$  and  $Sun_{\text{sum}}$  and the mean temperatures of winter and the number of sunshine hours of summer, respectively. Though showing a weak positive direct effect on growth, MEI was linked to stronger negative indirect effects and has a resulting negative total effect on tree ring growth ( $r_{\text{direct}} = 0.05$ ,  $r_{\text{indirect}} = -0.22$ ,  $r_{\text{total}} = -0.17$ ) in this species. Conversely, the positive indirect effect of EAWM through  $T_{\text{win}}$  reinforced its positive direct effect on *S. superba* growth ( $r_{\text{direct}} = 0.19$ ,  $r_{\text{indirect}} = 0.24$ ,  $r_{\text{total}} = 0.43$ ).

#### Growth projections for long-term trends

Three prediction models were successfully verified by showing statistical significance in the correlation test, sign test and the reduction of error for both early (1958–1983) and late periods (1984–2008; Table 5). All correlations were significant, and sign tests indicated that a significant association exists because the number of similarities (same sign either + or -) was significantly larger than the number of dissimilarities (opposite directions + and -, or - and +). In addition, all reduction of error (RE) values were positive, indicating that a statistical agreement between observed and predicted growth data was recognized for both early and late periods. The three models were therefore presumed to be stable and to accurately predict long-term growth trends; a predictive model was constructed using the full timespan comprising the early and late periods.

MEI and selected local climate factors were chosen in the regression models to predict tree growth in our three target taxa towards the end of this century as follows.

For *P. massoniana*,

$$\text{growth} = 0.380 - 0.046 \times T_{\text{win}} + 0.066 \times T_{\min(\text{atu})} - 0.085 \times \text{MEI}, \quad (1)$$

with an adjusted  $R^2 = 0.33$ ,  $i = 8.86$ ,  $P < 0.001$ .

**Table 4** Correlation between radial growth of the three species analyzed here and large-scale climatic factors

	MEI	EAWM	EASM	SASM
<i>Pinus massoniana</i>	-0.40**	0.30*	0.18	0.11
<i>Castanopsis eyrei</i>	0.01	-0.22	0.07	0.09
<i>Schima superba</i>	-0.17	0.41**	0.13	0.01

*MEI* annual mean of the Multivariate El Niño-Southern Oscillation Index, *EAWM* East Asia Winter Monsoon Index, *EASM* East Asia Summer Monsoon Index, *SASM* South Asian Summer Monsoon Index

\*  $P < 0.05$ , \*\*  $P < 0.01$

For *C. eyrei*,

$$\text{growth} = -1.134 + 0.040 \times T_{\min(\text{spr})} + 0.073 \times T_{\min(\text{sum})}, \quad (2)$$

with an adjusted  $R^2 = 0.21$ ,  $i = 7.32$ ,  $P = 0.002$ .

For *S. superba*,

$$\text{growth} = 1.116 - 0.088 \times T_{\text{win}} + 0.009 \times \text{Sun}_{\text{sum}}, \quad (3)$$

with an adjusted  $R^2 = 0.39$ ,  $i = 17.87$ ,  $P < 0.001$ .

Using these regression models, annual growth of *P. massoniana* in this century would show no change under the RCP 4.5 scenario ( $a = -5.67E - 5$ ,  $P = 0.813$ ), but significantly increase under the RCP 8.5 scenario ( $a = 0.0007$ ,  $P = 0.005$ ) (Fig. 5). For *C. eyrei*, the growth significantly increases both under the RCP 4.5 ( $a = 0.0026$ ,  $P < 0.0001$ ) and the RCP 8.5 ( $a = 0.0064$ ,  $P < 0.0001$ ) scenarios. Conversely, growth of *S. superba* is predicted to be reduced significantly both under the RCP 4.5 ( $a = -0.0021$ ,  $P < 0.0001$ ) and the RCP 8.5 ( $a = -0.0045$ ,  $P < 0.0001$ ) scenarios.

## Discussion

### Influence of local climatic conditions on tree growth

Our results indicate that the current summer temperatures in the study area are below the thermal growth optimum for *C. eyrei*, with rising temperatures predicted to stimulate this species' growth. Additionally, an increase in spring temperatures may trigger an early thaw and thereby prolong the growing season for *C. eyrei*, while low spring temperatures appear to increase the chilling damage to roots and delay the onset of this species' growth (Shi et al. 2010; Duan et al. 2012). The negative response of the other two tree species to increased winter temperatures indicate a more complex growth response to overall temperature increases. In *S. superba*, high winter temperature might enhance the tree's respiration rate, thus increasing consumption levels of carbohydrates otherwise available for growth (Gea-Izquierdo et al. 2012) which could explain the reduced growth rate. Furthermore, *S. superba* appears to benefit from increasing summer sun-

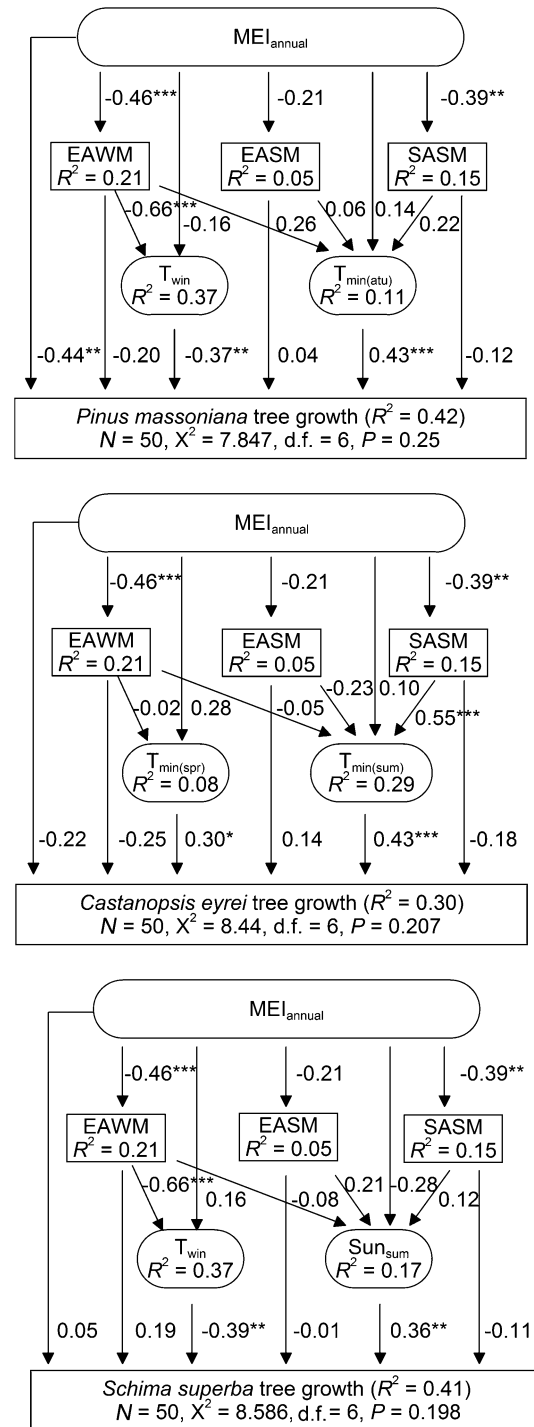


**Fig. 4** Path diagram showing direct and indirect influences of the El Niño-Southern Oscillation (ENSO) and Asian monsoon on the radial growth of the three coexisting tree species (\* $P < 0.05$ , \*\* $P < 0.01$ , \*\*\* $P < 0.001$ ). *MEI*<sub>annual</sub> annual value of the Multivariate ENSO Index, *EAWM* East Asian winter monsoon index, *EASM* East Asian summer monsoon index, *SASM* South Asian summer monsoon index,  $T_{\text{win}}$  mean temperatures of winter,  $T_{\min(\text{spr})}$  mean minimum temperature of spring,  $T_{\min(\text{sum})}$  mean minimum temperature of summer,  $T_{\min(\text{aut})}$  mean minimum temperature of autumn,  $\text{Sun}_{\text{sum}}$  sunshine hours of summer

**Table 5** Verification of predictive models for tree-ring width indices of *Pinus massoniana*, *Castanopsis eyrei* and *Schima superba*

Species	Calibration periods	Adjusted $R^2$	Correlation coefficient $R$	Sign test ( $\pm$ )	Reduction of error
<i>Pinus massoniana</i>	1958–1983	0.231	0.662**	18/7*	0.257
	1984–2008	0.396	0.562**	20/6**	0.178
<i>Castanopsis eyrei</i>	1958–1983	0.149	0.455*	17/8*	0.105
	1984–2008	0.255	0.565**	18/8*	0.210
<i>Schima superba</i>	1958–1983	0.338	0.630**	17/8*	0.140
	1984–2008	0.359	0.609**	21/5**	0.308

\*  $P < 0.05$ , \*\*  $P < 0.01$

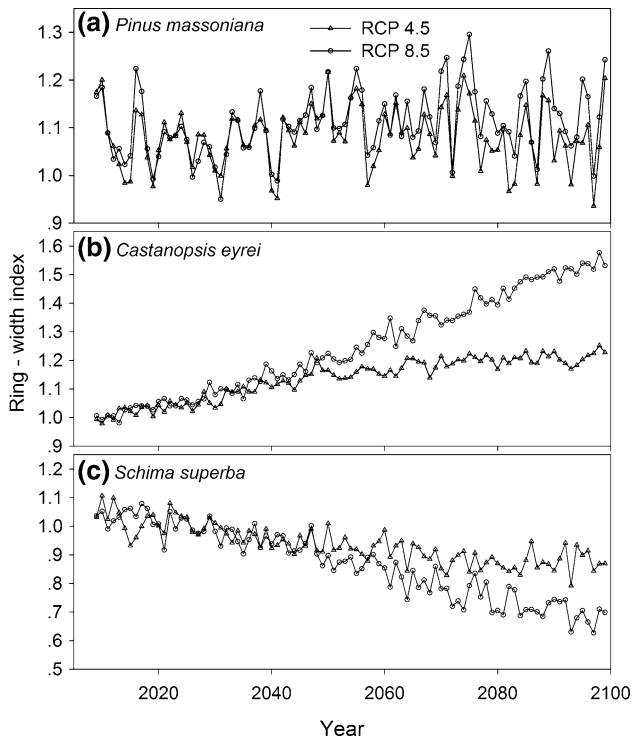


**Fig. 5** Temporal variation in growth rates of *Pinus massoniana*, *Schima superba*, and *Castanopsis eyrei* under the two sets of Representative Concentration Pathway scenarios (RCP 4.5 and RCP 8.5, respectively)

shine. While this factor is very difficult to model, the percentage of sunshine will potentially decrease when higher evapotranspiration rates caused by high summer temperatures lead to greater cloud cover and precipitation levels. Such correlations among climate variables highlight the importance of including all relevant climatic factors simultaneously in climate-growth models. In *P. massoniana*, which showed the most pronounced negative reaction toward increasing winter temperatures, this reaction might actually be overcompensated for by the species' increased growth during a prolonged growing season, reflected by the positive correlation with  $T_{\min(\text{aut})}$  (Piao et al. 2007). In general, the radial growth of the three species responds differently to climate change, partly be-

cause of their varying shade tolerance (successional status, Bazzaz and Miao 1993; Kerstiens 2001; Khurana and Singh 2004; Jones et al. 2009; De Oliveira et al. 2012; Villagra et al. 2013). Previous studies have reported that the ecophysiological characteristics of the dominant species of EBFs are strongly correlated with their successional status (Ding and Song 1998, 1999). However, additional study will be required to determine how these ecophysiological traits respond in global change scenarios.

While tree growth appears to be clearly associated to climatic drivers, the differential response of the three investigated species indicates that a strong need exists to determine climate-growth relationships for all important forest tree species in the varying subtropical forest types. Long-term datasets related to growth and climate are essential in this respect (Zhou et al. 2013), and tree ring analysis appears to be a very powerful basis for this type of analysis in subtropical areas (Morales et al. 2004; Barichivich et al. 2009; Chen et al. 2012; Duan et al. 2012; Guan et al. 2012; Zheng et al. 2012).

#### Large-scale climatic effects on tree growth

The ENSO and Asian monsoon exert a strong influence on precipitation, surface air temperatures, the intensity and number of storm events, moisture transport and atmospheric pressure in China (Huang et al. 2012). Together, these factors play a significant role in controlling the physiological processes that determine tree growth rates. The influence of ENSO on tree growth acts primarily via its effect on the Asian monsoon and local climatic factors. The large direct effect of ENSO on *P. massoniana* growth highlights that tree growth in some species can also be directly explained by the occurrence and severity of ENSO events. Although these direct effects were generally more important than indirect effects, our data indicate that in some cases the indirect influence of a climate index also played an important role in predicting growth patterns. For this reason, integrating the direct and indirect effects of ENSO and the Asian monsoon on local climatic conditions appears to be crucial to developing a mechanistic model of community dynamics under progressing climate change (Brienen et al. 2010; Pasho et al. 2011).



The detection of a relatively strong direct link between ENSO and *P. massoniana* growth has also been reflected by other studies in subtropical evergreen forests (Barichivich et al. 2009; Guan et al. 2012). This indicates that dendroclimatological reconstructions of ENSO events can be achieved in subtropical areas, potentially in terms of leading to more reliable predictions of the effects of climate change on tree growth.

#### Future climate change responses in tree ring growth

For *S. superba*, a strong negative response to climate change towards the end of this century linked to an overall reduction in tree growth is expected. In contrast, *C. eyrei* is more likely to profit from the predicted changes. Over longer time periods, the species-specific growth responses to climate change in our study will likely lead to shifts in the overall competitive balance among the coexisting tree species, triggering changes in the composition of the forest community and in the course of succession dynamics (Anderson-Teixeira et al. 2013; Zhou et al. 2013). Consequently, it is necessary to consider the functional differences among the coexisting species to predict the responses of the EBF to climate change. However, determining what limits growth of each coexisting species is a huge challenge in the subtropical EBF, reflected in the relatively low adjusted  $R^2$  of the dendrochronological regression models. Relationships between tree-ring widths and climatic factors are not always linear (Leonelli et al. 2009). Therefore, further improvement of predictive models will be important for improving the accuracy of predictions. In addition, great uncertainty exists in relation to the effects of future climate change on radial growth of the three species as predicted by our models, not in a small part because the regression models poorly represent other potential growth-limiting factors such as tree age and size, competition, genetic constraints, elevated  $\text{CO}_2$  and nutrient supply. At present, our knowledge on climate-growth and climate-survival relationships of subtropical trees is insufficient to make inferences about the community-wide responses of the EBF to climatic change. In addition, further studies are needed to quantify the contribution of other environmental factors aside from climate change, such as nitrogen deposition or the direct effects of rising concentrations of atmospheric  $\text{CO}_2$  on the composition of the EBF and related succession dynamics (Yu et al. 2014).

**Acknowledgments** The Natural Science Foundation of China (Grant No. 31270496), the Strategy Pioneer Sci-Tech Special Program, Chinese Academy of Science (Grant No. XDA05050203-02), the China Bureau of Foreign Experts and the Ministry of Education of China ("111" Program, Grant No. 2008-B08044) and the Grand Program on Global Change Research in China (Grant No. 2010CB951300) financially supported this research. We are grateful to two anonymous reviewers for their constructive criticism, suggestions, and comments, which resulted in a significantly improved manuscript.

## References

- Anderson-Teixeira KJ, Miller AD, Mohan JE, Hudiburg TW, Duval BD, DeLucia EH (2013) Altered dynamics of forest recovery under a changing climate. *Glob Change Biol* 19:2001–2021
- Ashton MS, Tyrrell ML, Spalding D, Gentry B (2012) *Managing forest carbon in a changing climate*. Springer, New York
- Babst F, Poulter B, Trouet V, Tan K, Neuwirth B, Wilson R, Carrer M, Grabner M, Tegel W, Levanic T (2013) Site- and species-specific responses of forest growth to climate across the European continent. *Glob Ecol Biogeogr* 22:706–717
- Barichivich J, Sauchyn DJ, Lara A (2009) Climate signals in high elevation tree-rings from the semiarid Andes of north-central Chile: responses to regional and large-scale variability. *Palaeogeogr Palaeoclimatol* 281:320–333
- Bazzaz FA, Miao SL (1993) Successional status, seed size, and responses of tree seedlings to  $\text{CO}_2$ , light, and nutrients. *Ecology* 74:104–112
- Bellenger H, Guilyardi E, Leloup J, Lengaigne M, Vialard J (2014) ENSO representation in climate models: from CMIP3 to CMIP5. *Clim Dynam* 42:1999–2018
- Brienen RJW, Lebrija-Trejos E, Zuidema PA, Martinez-Ramos M (2010) Climate-growth analysis for a Mexican dry forest tree shows strong impact of sea surface temperatures and predicts future growth declines. *Glob Change Biol* 16:2001–2012
- Chen F, Yuan Y, Wei W, Yu S, Zhang T (2012) Reconstructed temperature for Yong'an, Fujian, Southeast China: linkages to the Pacific Ocean climate variability. *Glob Planet Change* 86:11–19
- Cook ER (1985) *A time series analysis approach to tree-ring standardization*. University of Arizona, Tucson
- De Oliveira EAD, Approbato AU, Legracie JR Jr, Martinez CA (2012) Soil-nutrient availability modifies the response of young pioneer and late successional trees to elevated carbon dioxide in a Brazilian tropical environment. *Environ Exp Bot* 77:53–62
- Development Core Team R (2011) *R: A language and environment for statistical computing*. R Foundation for Statistical Computing, Vienna
- Ding S, Song Y (1998) Declining causes of *Pinus massoniana* in the processes of succession of evergreen broad-leaved forest. *Acta Bot Sin* 40:755–760
- Ding S, Song Y (1999) The comparison of photosynthesis physiology of evergreen broad-leaved forest of Tiantong National Forest Park in Zhejiang Province, China. *Acta Ecol Sin* 19:318–323
- Duan J, Zhang Q, Lv L, Zhang C (2012) Regional-scale winter-spring temperature variability and chilling damage dynamics over the past two centuries in southeastern China. *Clim Dynam* 39:919–928
- Fritts HC (1976) *Tree rings and climate*. Academic Press, London
- Galvan JD, Camarero JJ, Ginzler C, Buntgen U (2014) Spatial diversity of recent trends in Mediterranean tree growth. *Environ Res Lett*. doi:10.1088/1748-9326/9/8/084001
- Gea-Izquierdo G, Fonti P, Cherubini P, Martin-Benito D, Chaar H, Cañellas I (2012) Xylem hydraulic adjustment and growth response of *Quercus canariensis* Willd. to climatic variability. *Tree Physiol* 32:401–413
- Girard F, Beaudet M, Mailly D, Messier C (2014) Integrating climatic response in competition dependent tree-level growth models for northern hardwoods. *Forest Ecol Manag* 323:138–147
- Guan BT, Wright WE, Chung CH, Chang ST (2012) ENSO and PDO strongly influence Taiwan spruce height growth. *For Ecol Manag* 267:50–57
- Guo Q (1994) Relationship between the variations of East Asian winter monsoon and temperature anomalies in China. *Q J Appl Meteorol* 5:218–225
- He J, Zhang Q, Bazzaz FA (2005) Differential drought responses between saplings and adult trees in four co-occurring species of New England. *Trees Struct Funct* 19:442–450

- Holmes RL (1983) Computer-assisted quality control in tree-ring dating and measurement. *Tree Ring Bull* 43:69–78
- Huang R, Chen J, Wang L, Lin Z (2012) Characteristics, processes, and causes of the spatio-temporal variabilities of the East Asian monsoon system. *Adv Atmos Sci* 29:910–942
- Huang J, Bergeron Y, Berninger F, Zhai L, Tardif JC, Denneler B (2013) Impact of future climate on radial growth of four major boreal tree species in the Eastern Canadian boreal forest. *PLoS One* 8:e56758
- Jones TA, Domke GM, Thomas SC (2009) Canopy tree growth responses following selection harvest in seven species varying in shade tolerance. *Can J For Res* 39:430–440
- Kerstiens G (2001) Meta-analysis of the interaction between shade-tolerance, light environment and growth response of woody species to elevated CO<sub>2</sub>. *Acta Oecol* 22:61–69
- Khurana E, Singh JS (2004) Response of five dry tropical tree seedlings to elevated CO<sub>2</sub>: impact of seed size and successional status. *New For* 27:139–157
- Kira T (1991) Forest ecosystems of east and southeast Asia in a global perspective. *Ecol Res* 6:185–200
- Kline RB (2010) Principles and practice of structural equation modeling. The Guilford Press, New York
- Legendre P, Mi X, Ren H, Ma K, Yu M, Sun IF, He F (2009) Partitioning beta diversity in a subtropical broad-leaved forest of China. *Ecology* 90:663–674
- Leonelli G, Pelfini M, Battipaglia G, Cherubini P (2009) Site-aspect influence on climate sensitivity over time of a high-altitude *Pinus cembra* tree-ring network. *Clim Change* 96:185–201
- Li J, Zeng Q (2002) A unified monsoon index. *Geophys Res Lett* 29:1274
- Li J, Zeng Q (2003) A new monsoon index and the geographical distribution of the global monsoons. *Adv Atmos Sci* 20:299–302
- Li Y, Zhou G, Zhang D, Wenigmann KO, Otieno D, Tenhunen J, Zhang Q, Yan J (2012) Quantification of ecosystem carbon exchange characteristics in a dominant subtropical evergreen forest ecosystem. *Asia-Pac J Atmos Sci* 48:1–10
- Liu H, Williams AP, Allen CD, Guo D, Wu X, Anenkhonov OA, Liang E, Sandanov DV, Yin Y, Qi Z, Badmaeva NK (2013) Rapid warming accelerates tree growth decline in semi-arid forests of Inner Asia. *Glob Change Biol* 19:2500–2510
- May RM (1974) On the theory of niche overlap. *Theor Popul Biol* 5:297–332
- Miyamoto Y, Griesbauer HP, Scott Green D (2010) Growth responses of three coexisting conifer species to climate across wide geographic and climate ranges in Yukon and British Columbia. *For Ecol Manag* 259:514–523
- Morales MS, Villalba R, Grau HR, Paolini L (2004) Rainfall-controlled tree growth in high-elevation subtropical treelines. *Ecology* 85:3080–3089
- Moss RH, Edmonds JA, Hibbard KA, Manning MR, Rose SK, Van Vuuren DP, Carter TR, Emori S, Kainuma M, Kram T (2010) The next generation of scenarios for climate change research and assessment. *Nature* 463:747–756
- Pan Y, Birdsey RA, Fang J, Houghton R, Kauppi PE, Kurz WA, Phillips OL, Shvidenko A, Lewis SL, Canadell JG (2011) A large and persistent carbon sink in the world's forests. *Science* 333:988–993
- Pasho E, Camarero JJ, de Luis M, Vicente-Serrano SM (2011) Impacts of drought at different time scales on forest growth across a wide climatic gradient in north-eastern Spain. *Agric For Meteorol* 151:1800–1811
- Piao S, Friedlingstein P, Ciais P, Viovy N, Demarty J (2007) Growing season extension and its impact on terrestrial carbon cycle in the Northern Hemisphere over the past 2 decades. *Glob Biogeochem Cycles* 21:GB3018
- Shi J, Cook ER, Lu H, Li J, Wright WE, Li S (2010) Tree-ring based winter temperature reconstruction for the lower reaches of the Yangtze River in southeast China. *Clim Res* 41:169
- Song K, Yu Q, Shang KK, Yang T, Da LJ (2011) The spatio-temporal pattern of historical disturbances of an evergreen broadleaved forest in East China: a dendroecological analysis. *Plant Ecol* 212:1313–1325
- Stevenson S, Fox-Kemper B, Jochum M, Neale R, Deser C, Meehl G (2012) Will there be a significant change to El Niño in the twenty-first century? *J Clim* 25:2129–2145
- Stevenson S, Rajagopalan B, Fox-Kemper B (2013) Generalized linear modeling of the El Niño/Southern Oscillation with application to seasonal forecasting and climate change projections. *J Geophys Res Oceans* 118:3764–3781
- Subedi N, Sharma M (2013) Climate-diameter growth relationships of black spruce and jack pine trees in boreal Ontario, Canada. *Glob Change Biol* 19:505–516
- Takahashi K, Okuhara I (2013) Forecasting the effects of global warming on radial growth of subalpine trees at the upper and lower distribution limits in central Japan. *Clim Change* 117:273–287
- Tan Z, Zhang Y, Schaefer D, Yu G, Liang N, Song Q (2011) An old-growth subtropical Asian evergreen forest as a large carbon sink. *Atmos Environ* 45:1548–1554
- Tan Z, Zhang Y, Liang N, Hsia YJ, Zhang Y, Zhou G, Li Y, Juang J, Chu H, Yan J (2012) An observational study of the carbon-sink strength of East Asian subtropical evergreen forests. *Environ Res Lett* 7:044017
- Taylor KE, Stouffer RJ, Meehl GA (2012) An overview of CMIP5 and the experiment design. *Bull Am Meteor Soc* 93:485–498
- Villagra M, Campanello PI, Montti L, Goldstein G (2013) Removal of nutrient limitations in forest gaps enhances growth rate and resistance to cavitation in subtropical canopy tree species differing in shade tolerance. *Tree Physiol* 33:285–296
- Wang X, Kent M, Fang X (2007) Evergreen broad-leaved forest in Eastern China: its ecology and conservation and the importance of resprouting in forest restoration. *For Ecol Manag* 245:76–87
- Way DA, Oren R (2010) Differential responses to changes in growth temperature between trees from different functional groups and biomes: a review and synthesis of data. *Tree Physiol* 30:669–688
- Weare BC (2013) El Niño teleconnections in CMIP5 models. *Clim Dynam* 41:2165–2177
- Williams AP, Allen CD, Millar CI, Swetnam TW, Michaelsen J, Still CJ, Leavitt SW (2010) Forest responses to increasing aridity and warmth in the south-western United States. *Proc Natl Acad Sci USA* 107:21289–21294
- Wills C, Harms KE, Condit R, King D, Thompson J, He F, Muller-Landau HC, Ashton P, Losos E, Comita L (2006) Nonrandom processes maintain diversity in tropical forests. *Science* 311:527–531
- Wolter K, Timlin MS (2011) El Niño/Southern Oscillation behaviour since 1871 as diagnosed in an extended multivariate ENSO index (MEI, ext). *Int J Climatol* 31:1074–1087
- Wu Z (1980) Vegetation of China. Science Press, Beijing
- Xing P, Zhang Q, Baker PJ (2012) Age and radial growth pattern of four tree species in a subtropical forest of China. *Trees Struct Funct* 26:283–290
- Yan J, Zhang Y, Yu G, Zhou G, Zhang L, Li K, Tan Z, Sha L (2013) Seasonal and inter-annual variations in net ecosystem exchange of two old-growth forests in southern China. *Agric For Meteorol* 182–183:257–265
- Yu G, Chen Z, Piao S, Penge C, Ciais P, Wang Q, Li X, Zhu X (2014) High carbon dioxide uptake by subtropical forest ecosystems in the East Asian monsoon region. *Proc Natl Acad Sci USA* 111:4910–4915
- Zheng Y, Zhang Y, Shao X, Yin Z, Zhang J (2012) Temperature variability inferred from tree-ring widths in the Dabie Mountains of subtropical central China. *Trees* 26:1887–1894
- Zhou G, Peng C, Li Y, Liu S, Zhang Q, Tang X, Liu J, Yan J, Zhang D, Chu G (2013) A climate change-induced threat to the ecological resilience of a subtropical monsoon evergreen broad-leaved forest in Southern China. *Glob Change Biol* 19:1197–1210
- Zhu Y, Zhao G, Zhang L, Shen G, Mi X, Ren H, Yu M, Chen J, Chen S, Fang T (2008) Community composition and structure of Gutianshan forest dynamic plot in a mid-subtropical evergreen broad-leaved forest, East China. *Plant Ecol* 32:262–273